

# The correlation between echographic and histopathological findings in uveal melanoma

Magdalena ŘEDINOVÁ-VOKROJOVÁ<sup>1</sup>, Josef ŠACH<sup>2</sup>, Ilona SOUČKOVÁ<sup>1</sup>,  
Drahomira BARÁKOVÁ<sup>1</sup>, Jana VRÁNOVÁ<sup>3</sup>, Pavel KUCHYNKA<sup>1</sup>

1. Department of Ophthalmology, 3<sup>rd</sup> Faculty of Medicine, Charles University
2. Institute of Pathology, 3<sup>rd</sup> Faculty of Medicine, Charles University
3. Institute of Biophysics, 3<sup>rd</sup> Faculty of Medicine, Charles University

Correspondence to: Magdalena Ředinová-Vokrojová, MD  
Department of Ophthalmology, 3<sup>rd</sup> Faculty of Medicine, Charles University  
Vinohrady Teaching Hospital, Šrobárova 50,  
100 34 Prague 10, Czech Republic  
TEL.: +420 267162390; MOBIL PHONE: +420 603287868  
EMAIL: redinova@fnkv.cz

Submitted: 2008-05-15 Accepted: 2008-06-20 Published online: 2008-08-30

Key words: **uveal melanoma; standardised echography; prognostic factors**

Neuroendocrinol Lett 2008; 29(4):536–546 PMID: 18766140 NEL290408A23 © 2008 Neuroendocrinology Letters • www.nel.edu

## Abstract

**PURPOSE:** To correlate between the echographic and histopathological findings, and to search for important criteria for the prognosis *in vivo* using standardised echography.

**METHODS:** The study included 51 consecutive patients treated by primary enucleation for choroidal or ciliary body melanoma and 30 patients who underwent secondary enucleation after failing radiotherapy treatment. All patients were treated during the period of 1998–2008 at the Eye Clinic of the 3<sup>rd</sup> Faculty of Medicine in Prague, Czech Republic. Standardised echography based on the Ossoinig method was used in this study. Histopathological processing and evaluation was performed by the Laboratory of Ocular Pathology at the same clinic. Professional statistical software (Statistica 7.1 by Statsoft, Inc.) was used for all statistical analysis.

**RESULTS:** Statistically significant results were found in these correlations in the group of primary enucleation: US prominence vs. HP prominence ( $R = 0.8943$ ,  $p = 0.0000$ ), US base vs. HP base ( $R = 0.8060$ ,  $p = 0.0000$ ), US tumor shape vs. HP tumor shape ( $R = -0.7576$ ,  $p = 0.0000$ ), posterior choroidal spike condition vs. scleral invasion ( $R = -0.5341$ ,  $p = 0.0005$ ), TNM vs. pTNM ( $R = 0.7242$ ,  $p = 0.0000$ ). In the group of secondary enucleation: US prominence vs. HP prominence ( $R = 0.8132$ ,  $p = 0.0000$ ), US base vs. HP base ( $R = 0.7959$ ,  $p = 0.0000$ ). Other correlations were statistically insignificant.

**CONCLUSIONS:** Tumor dimensions, shape of the tumor and scleral invasion are important predictors that can be *in vivo* reliably determined using standardised echography.

## INTRODUCTION

Uveal melanoma is the most common primary intraocular malignant tumor in adults with metastatic potential [10, 16].

The incidence of uveal melanoma in Europe is 2–7 new cases per year per million people [4].

Standardised echography is one of the most important diagnostic methods in the differential diagnosis of intraocular tumors [1, 2, 3, 10, 18]. Whereas in clear optical media standardised echography provides crucial supportive evidence of a uveal melanoma, in eyes with opaque media, it is vital in the diagnosis. Apart from its diagnostic value, it is extremely important for measuring the size of the tumor accurately and assessing the extraocular invasion of the tumor. The accurate assessment of tumor size is critical for tumor staging, treatment selection and brachytherapy or other types of radiotherapy planning [1, 2, 6, 17]. When using brachytherapy, standardised echography can be used to check the position of radiotherapy plaque. It is also an important method for the assessment of regression or possible progression of the tumor after radiotherapy [10, 16].

Standardised echography was introduced in the 1960's by Ossoinig for the purpose of ophthalmic-tissue differentiation. The term standardised echography includes using the combination of standardized A-scan and real time contact B-scan [1].

The B-scan is used to determine the topographic features of lesions, such as shape, localization, and extension. The A-scan is used to determine the structure, reflectivity, vascularity at the tissue-sensitivity level and to measure the prominence [1, 7, 14, 15].

Apart from providing topographical information a B-scan is used to measure the longest basal diameter – in longitudinal and transversal sections – and prominence. Nevertheless, the standardised A-scan provides more accurate measurements of prominence using a decreased gain (in db) level to distinguish the surface of the tumor and the intrascleral spikes.

Recent studies of standardised echography reported the following echographic characteristics of uveal melanoma: low to medium reflectivity (5–60% spike height), regular internal structure, mushroom or dome shape, sound attenuation and internal vascularity.

Numerous studies support the importance of prognostic factors and the direct impact of these factors on survival rates in patients with uveal melanoma [5, 13, 16, 21]. Cell type, tumor size and extrascleral extension are the most important predictors of survival. Other factors, such as location of the tumor, gross shape of the tumor and features of local invasion (Bruch's membrane rupture, retinal invasion, presence of tumor cells in vitreous, invasion of emissary canals and invasion of vortex veins) and mitotic activity, are described as prognostic. The lymphocytic infiltration and specific vessel loops in the tumor are also often considered important for the prognosis.

The goal of our research was to compare the results of an ultrasonic examination with histopathological measurements. Furthermore, we focused on the presence of prognostic factors detectable *in vivo* using standardised echography.

## MATERIAL AND METHODS

The study included 51 consecutive patients treated by primary enucleation for choroidal or ciliary body melanoma and 30 patients who underwent secondary enucleation after failing radiotherapy treatment. All patients were treated during the period of 1998–2008 at the Eye Clinic of the 3<sup>rd</sup> Faculty of Medicine in Prague, Czech Republic.

All patients underwent enucleation.

The average age of diagnosis in women was 60.72 years (range 33–78); in men it was 56.39 years (range 27–80).

The patients in the group of secondary enucleation underwent brachytherapy using of ruthenium plaque applicator (56.7%), Leksell gamma-knife therapy (33.3%) or both (10.0%). Enucleation was performed in 6 cases (20.0%) because of treatment complications (secondary glaucoma) and in 24 cases (80%) because of radiotherapy failure.

### Echographic examination

All patients (their tumors) were evaluated using standardised echography based on the Ossoinig method. The examinations were performed using Ophthascan S Mini A, Ophthascan B (Alcon Biophysic Medical) and Cinescan S (Quantel Medical).

The A-mode transducer had the following specifications: nominal frequency of 8 MHz, non-focused probe and a diameter of 5 mm. The B-mode transducer had the following specifications: mechanical sector scanning, frame rate 10–12 Hz, nominal frequency of 10 MHz, focused probe and focus at 20 mm from exit window of scan head.

The examinations were performed by two experienced examiners.

The contact method was used, with the scanning probe placed on the conjunctiva, opposite the tumor. The immersion method with a scleral shell was used for examining tumors involving anterior segment structures.

Topical anaesthesia was used with tetracain (0.5–1.0%) or oxybuprocain (Novesin 0.4% gtt) and was applied before the examination.

*The following sonographic features were:* tumor shape, reflectivity, regularity – internal structure, sound attenuation, irregularity of posterior choroidal spike, extra-scleral extension, and measurement (prominence, base diameter).

### **Tumor shape**

After describing the shape of the tumor using B-mode, the tumors were classified and divided into the following groups: dome-shaped, mushroomed and lobulated.

### **Reflectivity**

Reflectivity quantifies the mean echo amplitude of the tumor in percentage of the maximum display height. A-scan was used for reflectivity assessment. The reflectivity was graded as low to medium (0–20%), medium to high (20–40%) and high (40–60%).

### **Vascularity of the tumor**

The A-Mode was used to evaluate the vascularity of the tumor. The vascularity is revealed by one or more echo peaks displaying a rapid vertical movement on the screen. The tumors were classified as vascularity positive or negative.

### **Regularity, internal structure of the tumor**

A- and B-Modes were used to evaluate the internal structure. The regularity is defined as the mode of distribution of peak amplitudes throughout the tumor. The tumors were divided into the following categories: regular structure or irregular structure.

### **Sound attenuation**

Sound attenuation is describes the decrease of ultrasonic energy absorbed by the tissue. It was evaluated using A-scan.

The tumors were classified into two groups: sound attenuation present or not present.

### **Scleral invasion**

Scleral invasion is suggested when the posterior choroidal spike and the steeply rising scleral spike are impossible to display. A-mode was used to determine the scleral invasion. The tumors were graded as follows: posterior choroidal spike regular or irregular.

### **Extrascleral extension**

The extrascleral extension was determined by both modes.

In case the scleral echo was not present and a lesion of the same echogenity as the primary tumor was found close to the sclera and connected with the base of the tumor, it was rated as a positive scleral extension.

Choroidal excavation was not included in this study, because the presence of choroidal excavation is not typical only for uveal melanoma. However, it can be found in other choroidal lesions.

### **Tumor size measurement**

The measurement of the prominence was performed using Ophthascan "S" Mini A (Alcon Biophysic Medical) with a level of tissue sensitivity of 67.4 dB, Cinescan S (Quantel Medical) with a level of tissue sensitivity 72,3 dB. The measurement was conducted using the

contact method. The non-focused 8 MHz probe with an ultrasonic velocity signal of 1550 m/s was used. The perpendicular orientation of the probe with respect to the tumor surface and sclera was verified by displaying double-peaked, steeply rising spikes from tumor and scleral surfaces. The distance between the spikes was measured using electronic cursors.

The measurement of the longest basal diameter, in both longitudinal and transversal section, was performed using Ophthascan Mini B (Alcon Biophysic Medical), and Cinescan S (Quantel Medical) with a focused 10 MHz probe.

### **Histopathological examination:**

Histopathological processing and evaluation was performed by the Laboratory of Ocular Pathology at the same clinic.

The eyes were fixed and histologically processed and sectioned according to a standard protocol. The gross examination and histological evaluation of the slides stained with hematoxylin- eosin (5 µm thick) was performed by an experienced ocular pathologist.

*The following morphological features were evaluated in every case:* cell type, tumor measurement (apical height, LTD), pigmentation, mitotic activity, localization of tumor, local invasion (invasion of the retina, optic nerve/optic disc invasion, tumor cell in vitreous, vortex vein invasion, invasion into emissary canals), scleral invasion and extrascleral extension.

In the secondary enucleation group we also described the vital signs of the tumor.

The cell type was categorized according to the classification decreed by Callender (1931) and in this study it was grouped into spindle A+B, spindle B, predominantly spindle B, mixed, epithelioid and predominantly epithelioid, and the category of complete tumor regression was described in the group of secondary enucleation.

The particular cell types are well described and defined in the literature. As a mixed type we classified the tumors in which the admixture of some other than the prevailing component (usually admixture of the epithelioid component) reached at least 20% of the tumor mass at the estimation.

Mitotic activity was evaluated in the tumor and the following categories were defined:

No mitotic activity – when no mitotic figures were observed within the tumor in the histological sections. Low mitotic activity – when up to 5 mitotic figures were observed on average within the tumor per 10 high power fields (HPF = visual field with microscopic objective 1:40). Medial mitotic activity – when 5–7 mitotic figures were observed on average within the tumor per 10 HPF. High mitotic activity – when more than 7 mitotic figures were observed on average within the tumor per 10 HPF.

The location of the tumor within the eye globe was classified into the following categories:

1. Posterior part of the choroid – located in the choroid behind the equator.
2. Anterior part of the choroid – tumors located in the choroid anteriorly from the equator or with the majority of their volume located anteriorly from the equator.
3. Ciliary body with anterior part of the choroid. Either the choroid or ciliary body can be involved secondarily, according to the growth and progression of the tumor. However, both parts of the uvea are infiltrated at the time of examination and the primary location cannot be reliably established. Only sometimes the tendency to the circular shape and the circular extension of the tumor points to the ciliary body as the more likely primary location.
4. Ciliary body – tumors located only within the ciliary body, without extension to other parts of the uvea.
5. Ciliary body and iris – involvement of the ciliary body and iris, otherwise analogous as in No. 3 – “ciliary body with anterior choroid”
6. Iris – tumors located only within iris, without involvement of the other parts of uvea.

#### Other local invasion of the tumor:

Deep scleral invasion – the growth of the tumor through the scleral emissaria, but without reaching the external surface of the sclera. We discerned the depth of this invasion within the sclera – none to 1/3, more than one third and the overall scleral thickness.

Intraluminal growth in the vorticosae vein, invasion of the anterior angle filtration structures, growth through Bruch’s membrane with invasion of the retina or even invasion into the vitreous were other possible kinds of local invasion which we had noticed.

The extraocular extension of the tumor – tumorous growth reaching the external surface of the sclera – either without grossly visible extrascleral tumorous focus (then microscopical extraocular extension), or with grossly visible extrascleral tumorous focus – (then macroscopical extraocular extension). The most common way for the extrascleral extension of the tumor is through emissarial channels. The extrascleral extension of the tumour was graded as follows: none, microscopic and macroscopic.

The pigmentation of the tumor was also evaluated for the purpose of possible other correlations. The following semiquantitative scale was established for this evaluation:

Low pigmentation – cases in which the pigment was observable within the tumorous cells, but only in minimal amount, requiring particular searching for it using high power magnification. Grossly, the colour of the tumor on the section was white to grey.

Medial pigmentation – pigmentation observable within the tumorous cells easily, without particular searching, with only low power magnification. However, the amount of pigment was still relatively small, without obscuring of the other microscopical details

within the tumor and tumorous cells. Grossly, the colour of the tumor on the section was light brown.

Heavy pigmentation – intensive pigmentation obscuring other microscopical details of the tumor and its cells, requiring bleaching of the histological sections with hydrogen peroxide for evaluation of the other microscopical details. Grossly, the colour of the tumor was dark brown or even brown to black.

Irregular (patchy) pigmentation – tumors with variable intensity of pigmentation within the degrees described above in the different areas of one tumor.

No pigmentation – totally without pigmentation in the tumor, even microscopically amelanotic forms of the uveal melanoma. The diagnosis of melanoma has to be confirmed immunohistochemically in these rare cases, with the positivity of HMB 45 and melan A markers.

#### Regression of the tumor:

In the group of secondary enucleation, we determined the regression of the tumor. The volume of vital tumorous tissue was compared with the volume of re-

**Table 1:** Echographic characteristics

	Group of primary enucleation (n=51)	Group of secondary enucleation) (before radiotherapy) (n=30)
<b>Tumor shape</b>		
Dome	32 (62.7 %)	20 (66.7%)
Mushroom	18 (35.3 %)	10 (33.3 %)
Lobulated	1 (2.0 %)	0
<b>Reflectivity</b>		
Low	10 (19.6%)	8 (26.7%)
Low to medium	34 (66.7%)	22 (73.3 %)
Medium to high	7 (13.7%)	0
<b>Internal structure</b>		
Regular	39 (76.5%)	24 (80%)
Irregular	12 (23.5%)	6 (20%)
<b>Vascularity</b>		
Positive	46 (90.2%)	19 (63.3%)
Negative	5 (9.8%)	11 (36.7%)
<b>Sound attenuation</b>		
Positive	51 (100%)	30 (100%)
Negative	0	0
<b>Scleral invasion</b>		
Posterior choroidal spike irregular	18 (35.3%)	6 (20%)
Posterior choroidal spike regular	33 (64.7%)	24 (80%)
<b>Extrascleral extension</b>		
Positive	0	0
Negative	51 (100%)	30 (100%)
<b>Retinal detachment</b>		
Positive	45 (88.2%)	25 (83.3%)
Negative	6 (11.8%)	5 (16.7%)

**Table 2:** Histopathological characteristics:

	Group of primary enucleation (n=51)	Group of secondary enucleation (n=30)
<b>Cell type:</b>		
Spindle B	25 (49%)	11 (36.7%)
Spindle A+B	2 (3.9%)	0
Mixed	6 (11.8%)	4 (13.3%)
Predominantly spindle B	15 (29.4%)	6 (20.0%)
Predominantly epithelioid	1 (2.0%)	1 (3.3%)
Epithelioid	2 (3.9%)	1 (3.3%)
totally regressed	-	7 (23.3%)
<b>Mitotic activity:</b>		
No	8 (15.7%)	25 (83.3%)
Low	37 (72.5%)	5 (16.7%)
Medial	6 (11.8%)	0
<b>Pigmentation:</b>		
Mild	15 (29.4%)	7 (23.3%)
Moderate	14 (27.4%)	5 (16.7%)
Heavy	18 (35.3%)	11 (36.7%)
Irregular	4 (7.8%)	0
Impossible to determine	0	7 (23.3%)
<b>Localization of tumor:</b>		
gr.1	25 (49.0%)	21(70.0%)
2	9 (17.6%)	2 (6.7%)
3	15 (29.4%)	6 (20.0%)
4	0	0
5	1 (2.0%)	1 (3.3%)
6	1 (2.0%)	0
<b>Invasion of Bruchs membrane:</b>		
Intact	17 (33.3%)	18 (60.0%)
Broken	34 (66.7%)	12 (40.0%)
<b>Local tumor invasion:</b>		
None	19 (37.3%)	20 (66.7%)
Invasion of the retina	17 (33.3%)	5 (33.3%)
Optic nerve/optic disc invasion	4 (7.8%)	2 (6.7%)
Tumor cell in vitreus	0	0
Vortex vein invasion	3 (5.9%)	1 (3.3%)
Invasion into emissary canals	2 (3.9%)	
Schlem. canal.	8 (15.7%)	2 (6.7%)
<b>Scleral invasion:</b>		
None -1/3	32 (62.7%)	21 (70.0%)
More than 1/3	19 (37.3%)	9 (30.0%)
<b>Extrascleral extension:</b>		
None	45 (88.2%)	29 (96.7%)
Microscopic	5 (9.8%)	1 (3.3%)
Macroscopic	1 (2.0%)	0

gressed tumor mass. The scared or necrotic tissue was considered as regressed tumorous mass. The rate between the volume of vital and regressed tumorous tissue was estimated on a semiquantitative scale: fully or nearly vital tumor (tumor vitality of 75–100%) minority of tumor regression (vitality of 50–75%), majority of tumor regression (vitality of 25–50%) and totally or nearly totally regressed (vitality of 0–25%).

On every enucleated globe, the bioptic prominence measurement and tumor basis measurement was performed using a slide gauge with vernier scale and 0.1 mm resolution on a dissected profixed globe (minimum of 5-days fixation in 5% formaldehyde). At the bioptic measurement, the distance between the inner sclera surface below the tumor and the retinal surface over the apical part of the tumor was measured as the maximum prominence. The tumor basis was measured as the distance between the most distant points on the transition between the tumor surface and surrounding globe surface.

## RESULTS

The results are summarised in Tables 1 and 2.

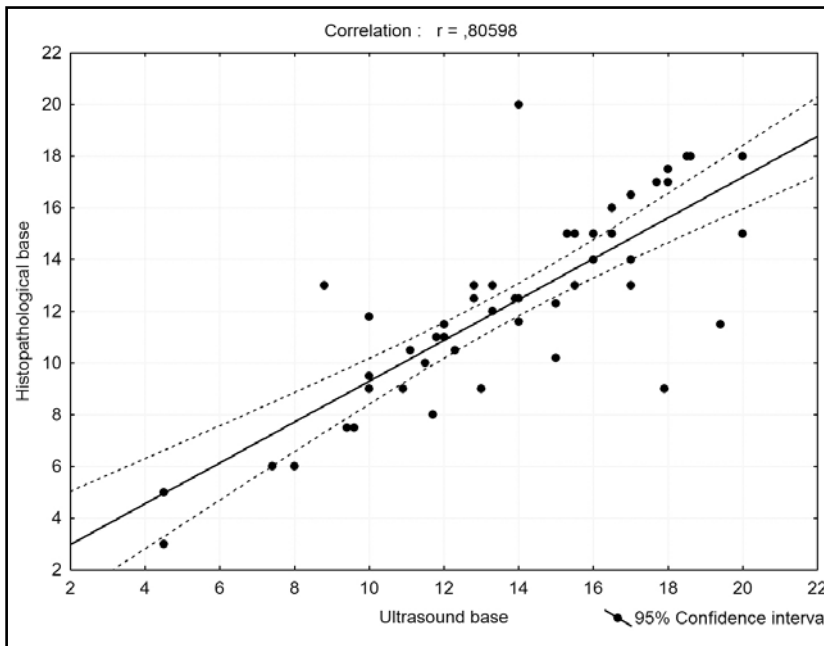
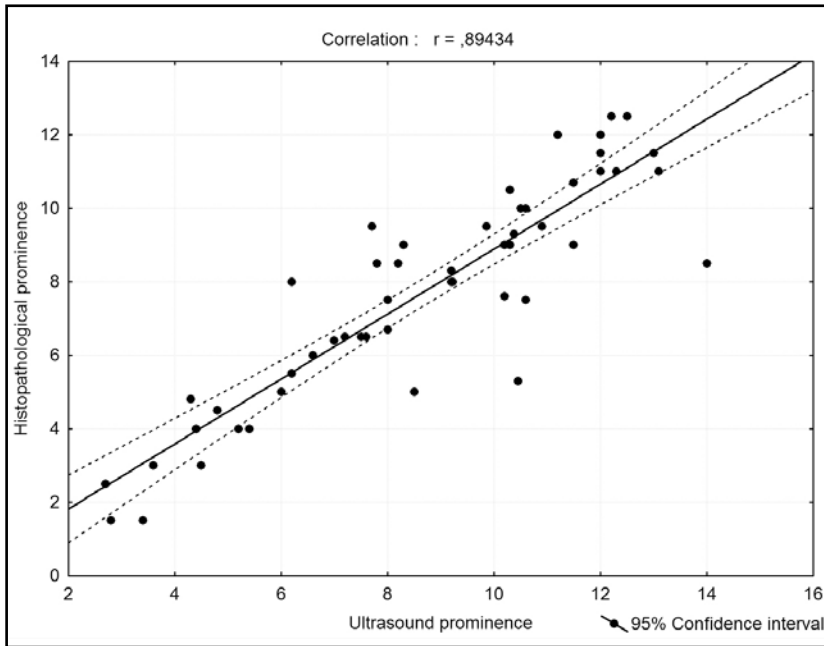
### Echographic characteristics:

#### *The group of primary enucleation*

The most common tumor shape was the dome (62.7%), followed by the mushroom (35.3%). Low to medium reflectivity was observed in 66.7%, followed by low reflectivity in 19.6%. The regular internal structure was observed in 80.4% of tumors, sound attenuation was observed in 100%, vascularity was observed in 90.2% of tumors, and secondary retinal detachment was observed in 88.2%. Scleral invasion was present in 35.3% of the tumors. The extrascleral extension was not present in this group. Tumor size was classified according to the Collaborative Ocular Melanoma Study criteria. In the group of primary enucleation, 21 (41.18%) were large-sized and 30 (58.82%) were medium-sized tumors.

#### *The group of secondary enucleation*

These results of ultrasonic examinations were found at the time when the tumor was diagnosed. The most common tumor shape was the dome in 66.7%, followed by the mushroom in 33.3%. Low to medium reflectivity was observed in 73.3%, followed by low reflectivity in 26.7%. Regular internal structure was observed in 80%, vascularity was observed in 63.3%, sound attenuation was observed in 100%, secondary retinal detachment was observed in 83.3% and in 20% the scleral invasion was observed. The extrascleral extension was not present in this group. In the group of secondary enucleation, 28 (93.3%)



were medium-sized tumors, 1 (3.3%) was small and 1 (3.3%) was a large-sized tumor.

In the group of secondary enucleation, an ultrasonic examination was focused on changes after previous radiotherapy. Reflectivity, internal structure, and vascularity were features of this evaluation.

The results are summarized in Table 3.

In the post-radiotherapy ultrasonic examination, we observed changes in the internal structure, the presence of internal regularity was observed in 80% of the pre-radiotherapy ultrasonic imagination, and after radiotherapy, we observed an irregular internal structure in 73%. Sound attenuation was observed in 100% of pre-radiotherapy and 50% of post-radiotherapy tumors.

## Histopathological characteristics

### Group of primary enucleation

The most common cell type was spindle B (49%), followed by predominantly spindle B (29.4%). Low mitotic activity was observed in 72.5%. The main tumor location was the posterior part of the choroid in 49.0%, followed by the ciliary body with the anterior part of the choroid in 29.4%. Heavy pigmentation was observed in 35.3%, followed by mild in 29.4%. Signs (excluding rupture of Bruch's membrane) of local invasion were present in 62.74%. Bruch's membrane was broken in 66.7%. Scleral invasion higher than 2/3 was observed in 37.3%. Microscopic extrascleral extension was observed in 9.8%, and macroscopic in 2.0%.

### Group of secondary enucleation

The most common cell type was spindle B (36.7%), followed by predominantly spindle B (20.0%). In 83.3%, we observed no mitotic activity; low mitotic activity was observed in 16.7%. The main tumor location was the posterior part of the choroid in 70.0%, followed by the ciliary body with the anterior part of the choroid in 20.0%. Heavy pigmentation was observed in 36.7%, followed by mild in 23.3%. Signs (excluding rupture of Bruch's membrane) of local invasion were present in 33.3%.

Bruch's membrane was broken in 40.0%. Scleral invasion higher than 2/3 was observed in 37.3%. Microscopic extrascleral extension was observed in 3.3%, no macroscopic lesion was observed.

### Regression of the tumor:

60% of the tumors were totally vital or nearly totally vital tumors, 30% were totally or nearly totally regressed, 6.7% were classified as majority of the tumor regression and 3.3% as minority of the tumor regression.

We determined the clinical TNM classification from an ultrasonic examination and from histopathological observation. We determined pTNM and we studied the correlation between them.

## Data Analysis

### Statistical methods

Our aim was to find and prove the correlation between echographic display variables and variables from histopathological findings. Professional statistical software (STATISTICA 7.1 by Statsoft, Inc.) was used for all statistical analysis, namely the Correlation Analysis model for continuous variables and the Crosstabulation/frequency tables for categorical variables.

### The correlation analysis

We searched for correlation in the following continuous variables: the US prominence size vs. the HP prominence size; the US base size vs. the HP base size, for both groups of patients, successively. We can see the Pearson ratio values with the basic descriptive statistics in Table 4 for primary enucleation patients and in Table 5 for secondary enucleation patients. We can see the resulting correlations for primary enucleation patients in Figures 1 and 2 and for secondary enucleation patients in Figures 3 and 4.

A very strong correlation between the prominences and bases in ultrasonic and histopathological examinations can be seen both from Tables 4 and 5, as well as from the following Figures.

### Crosstabulations/ frequency tables

#### Primary enucleation

Frequency table analysis helps to analyse the relationship between the qualitative or discrete magnitudes. This method was first used for the primary enucleation group. We observed the following magnitudes:

- Ultrasound: tumor shape [dome-shaped, mushroomed, lobulated] vs. histopathology: tumor shape [dome-shaped, mushroomed, lobulated]
- Ultrasound: Posterior choroidal spike condition [regular, irregular] vs. histopathology: Scleral invasion [the invasion lower or equal to 1/3, invasion higher than 1/3]
- Ultrasound: reflectivity [low, medium, high] vs. Histopathology:
  - Cell cytology regarding Callender [group A: spindle B and spindle A+B, group B: mixed and predominantly spindle B, group C: epithelioid and predominantly epithelioid]
  - Mitotic activity [none, low, medial]
  - Pigmentation [low, medial, heavy, irregular]
- Ultrasound: internal structure [regular, irregular] vs. Histopathology:
  - Cell cytology regarding Callender [group A: spindle B and spindle A+B, group B: mixed and predominantly spindle B, group C: epithelioid and predominantly epithelioid]
  - Mitotic activity [none, low, medial]
  - Pigmentation [low, medial, heavy, irregular]
- Ultrasound :TNM vs. Histopathology: pTNM

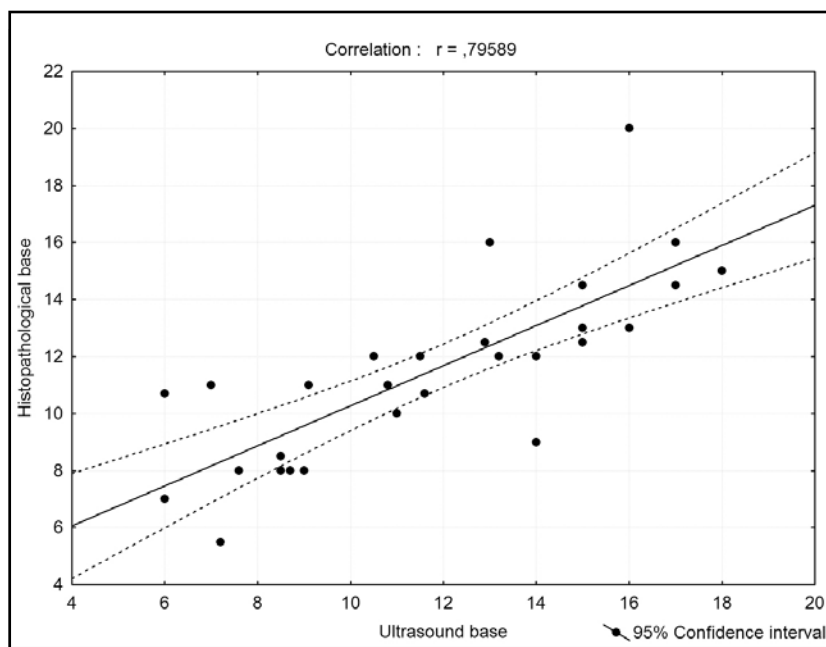
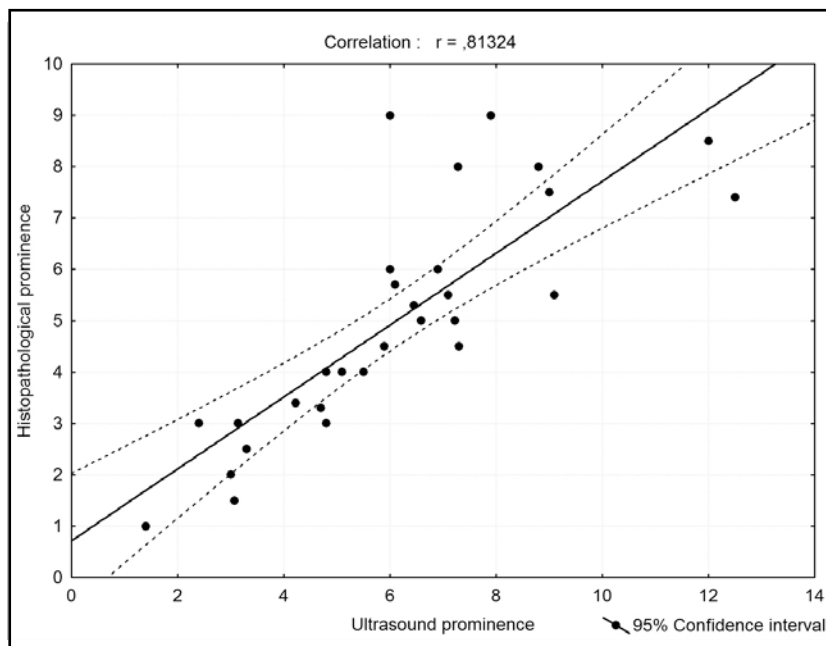


**Table 3:** Echographic characteristics before and after radiotherapy

	<b>Group of secondary enucleation when diagnosed (n=30)</b>	<b>Group of secondary enucleation before enucleation (n=30)</b>
<b>Reflectivity</b>		
Low	8 (26.7%)	6 (20.0%)
Low to medium	22 (73.3 %)	17(56.7%)
Medium to high	0	7 (23.3%)
<b>Internal structure</b>		
Regular	24 (80%)	8 (26.7%)
Irregular	6 (20%)	22 (73.3%)
<b>Vascularity</b>		
Positive	19(63.3%)	10(33.3%)
Negative	11 (36.7%)	20 (66.7%)
<b>Sound attenuation</b>		
Positive	30(100%)	15 (50%)
Negative	0	15 (50%)
<b>Scleral invasion</b>		
Posterior choroidal spike irregular	6 (20%)	8 (26.7%)
Posterior choroidal spike regular	24 (80%)	22 (73.3%)
<b>Extrascleral extension</b>		
Positive	0	0
Negative	0	0
<b>Retina detachment</b>		
Positive	25 (83.3%)	10(33.3%)
Negative	5 (16.7%)	20 (66.7%)

**Table 4:** Pearson correlation coefficient, determinant coefficient in the group of primary enucleation. (n=50)

<b>Variable X &amp; Y</b>	<b>Mean ± SD</b>	<b>R</b>	<b>R<sup>2</sup></b>	<b>T</b>	<b>p</b>
<b>Prominence ultrasound Prominence histopatholog.</b>	8.65 ± 2.99 7.70 ± 2.96	<b>0.8943</b>	<b>0.7999</b>	<b>13.9934</b>	<b>0.0000</b>
<b>Base ultrasound Base histopatholog.</b>	13.66 ± 3.78 12.19 ± 3.70	<b>0.8060</b>	<b>0.6500</b>	<b>9.4332</b>	<b>0.0000</b>

**Table 5:** Pearson correlation coefficient, determinant coefficient in the group of secondary enucleation. (n=29)

<b>Variable X &amp; Y</b>	<b>Mean ± SD</b>	<b>R</b>	<b>R<sup>2</sup></b>	<b>t</b>	<b>p</b>
<b>Prominence ultrasound Prominence histopatholog.</b>	6.12 ± 2.61 5.0 ± 2.25	<b>0.8132</b>	<b>0.6614</b>	<b>7.2616</b>	<b>0.0000</b>
<b>Base ultrasound Base histopatholog.</b>	11.93 ± 3.68 11.63 ± 3.25	<b>0.7959</b>	<b>0.6334</b>	<b>6.8307</b>	<b>0.0000</b>

**Table 6:** Contingence tables, homogeneity test and Spearman ratio for discrete magnitudes of ultrasonic and histopathological examinations (primary enucleation), (n=51)

The shape of the tumor	The shape of the tumor			Statistical coeff.	
	domeshaped	mushroomed	lobulated	Pearson coeff. X <sup>2</sup>	Spearman coeff. R
Domeshaped	31	1	0	<b>93.53013</b> sv = 4 <b>p = 0.0000</b>	<b>-0.7576</b> t = 8.124 <b>p = 0.0000</b>
Mushroomed	1	17	0		
Lobulated	0	0	1		

Posterior choroidal spike condition	Scleral invasion		Statistical coeff.	
	None to one third	More then one third	Pearson coeff. X <sup>2</sup>	Spearman coeff. R
Spike regular	27	6	<b>14.5509</b> sv= 1 <b>p = 0.00014</b>	<b>-0.5341</b> t = 4.423 <b>p = 0.0005</b>
Spike irregular	5	13		

Reflectivity	Cell type			Statistical coeff.	
	A	B	C	Pearson coeff. X <sup>2</sup>	Spearman coeff. R
Low to medium	6	3	1	1.25261 sv = 4 <b>p = 0.8694</b>	-0.0741 T = 0.5435 <b>p = 0.5893</b>
Medium to high	17	15	2		
High	4	3	0		

Reflectivity	Mitotic activity			Statistical coeff.	
	low	medial	none	Pearson coeff. X <sup>2</sup>	Spearman coeff. R
Low to medium	6	2	2	2.8832 sv = 4 <b>p = 0.5776</b>	0.1255 T = 0.8852 <b>p = 0.3804</b>
Medium to high	26	4	4		
High	5	0	2		

Reflectivity	Pigmentation				Statistical coeff.	
	low	medial	heavy	irregular	Pearson coeff. X <sup>2</sup>	Spearman coeff. R
Low to medium	1	2	7	0	8.2021 sv = 6 <b>p = 0.2237</b>	-0.1994 t = 1.424 <b>p = 0.1607</b>
Medium to high	11	11	9	3		
High	3	1	2	1		

Regularity (Internal stucture)	Cell type			Statistical coeff.	
	A	B	C	Pearson coeff. X <sup>2</sup>	Spearman coeff. R
Irregular structure	9	2	1	3.8919 sv = 2 <b>p = 0.1429</b>	0.2131 T = 1.5267 <b>p = 0.1333</b>
Regular structure	18	19	2		

Regularity (Internal stucture)	Mitotic activity			Statistical coeff.	
	low	medial	none	Pearson coeff. X <sup>2</sup>	Spearman coeff. R
Irregular structure	10	1	1	0.9495 sv = 2 <b>p = 0.6221</b>	0.1364 T = 0.9637 <b>p = 0.3399</b>
Regular structure	27	5	7		

Regularity (Internal stucture)	Pigmentation				Statistical coeff.	
	low	medial	heavy	irregular	Pearson coeff. X <sup>2</sup>	Spearman coeff. R
Irregular structure	2	4	6	0	3.2568 sv=3 <b>p = 0.3537</b>	0.1350 t = 0.9537 <b>p = 0.3449</b>
Regular structure	13	10	12	4		

TNM (US)	pTNM		Statistical coeff.	
	T1+T2	T3 + T4	Pearson coeff. X <sup>2</sup>	Spearman coeff. R
T1 +T2	25	0	<b>26.7483</b> sv=1 <b>p = 0.0000</b>	<b>0.7242</b> t = 7.3515 <b>p = 0.0000</b>
T3 + T4	8	18		

US – ultrasound

The basic enter data and the results of homogeneity tests, independence tests and the Spearman ratio R are stated in Table 6.

From the previous tables, we can see that a statistically relevant correlation, or statistically relevant Spearman ratio R value comparing the echographic and histopathological examinations, are at the following magnitudes:

- US tumor shape vs. HP tumor shape, ( $R = -0.7576$ ,  $p = 0.0000$ ),
- Posterior choroidal spike condition vs. Scleral invasion, ( $R = -0.5341$ ,  $p = 0.0005$ ),
- TNM vs. pTNM ( $R = 0.7242$ ,  $p = 0.0000$ )

## DISCUSSION

The cell type, size of the tumor, and presence of the extrascleral extension are the most reliable prognostic predictors regarding the mortality of patients with uveal melanoma. Although the cell type remains one of the most reliable predictors, its practical usability decreases with implementing alternative non-surgical therapeutic approaches. For this reason, the size of a tumor becomes currently the most usable and important prognostic predictor. As we have documented in our study, the size of a tumor can be reliably measured by standardized echography.

The accurate assessment of tumor size is critical for classification of tumor stadium, treatment selection, and the planning of brachytherapy/radiotherapy.

Our results regarding tumor-size measurement are similar to those published in COMS Report 21 (3), or those published by Nicholson (8) and by Marchini (24). The difference between the ultrasonic and the histopathological measurement of the tumor prominence does not exceed 1 mm. The generally accepted explanation for this difference is tumor shrinkage caused by fixation of the tumor before its measurement in the histopathological laboratory.

There are several explanations of the difference between results of the ultrasonic and bioptic measurements. The ultrasonic measurement is performed on the vital tumor with blood perfusion and without previous fixation, while the bioptic measurement is performed on the eyeball separated from blood flow, with at least partially collapsed blood vessels inside of the tumor. The coagulation of the proteins and partial dehydration of the tumor started by formalin fixation may also contribute to tumor shrinkage before the bioptic measurement [8, 9, 24].

As our study shows, there is no difference in the measurement of a tumor that underwent previous radiotherapy and the one that didn't.

Studies focused on the assessment of interobservers' variability, have shown good reproducibility of echographic measurement [11].

The shape of the tumor informs us about the condition of Bruch's membrane. The rupture of Bruch's membrane is an important prognostic factor too. The correlation between the echographic and the histopathological characteristics was highly statistically significant.

To detect scleral and extrascleral invasion, some studies prefer an MRI to a standardised echography examination, as the latter is less sensitive.

According to Scott [20], the use of standardised echography for extrascleral invasion was more sensitive than MRI. Moreover, Farah and Byrne [12] describe the detection of minimal scleral invasion of the tumor (25% of scleral thickness invasion) using standardised echography.

The results of this study prove that sclera infiltration can be found by standardised echography which is in correlation with a histopathological examination. However, the detection of scleral invasion is only possible when more than one third of scleral thickness is infiltrated, as the results show.

The detection of scleral invasion using standardised echography requires an experienced examiner [22, 23]. The follow-up examinations are also very important in order to detect changes in the tumor.

## CONCLUSIONS

The correlation between the ultrasonic reflectivity level and internal regularity of the tumor and histopathological findings, was statistically insignificant in our study. These results are similar to those described by COMS Report No. 29 [2], and Rosa [19].

According to our results, reflectivity and internal regularity cannot be used as a prognostic factor. Scleral invasion could only be detected when at least 1/3 of sclera thickness was infiltrated in the tumor. However, the tumor dimensions, the shape of the tumor and scleral invasion are predictors, which can be *in vivo* reliably determined using standardised echography.

TNM stated by using the standardised echography correlates with the histopathological TNM.

Our findings support the opinion that standardised echography can play a major role in confirming the diagnosis, obtaining accurate and reliable measurements and monitoring lesion changes over time. Standardised echography is an instrumental method for intraocular, scleral, and extrascleral extension.

REFERENCES

- 1 Ossoinig KC (1979). Standart echography. Basic principles, clinical applications and results. *Int.Ophthalmol.Clin.***19**: 127–219.
- 2 Collaborative Ocular Melanoma Study Group. Baseline Echographic Characteristics of Tumours in Eyes of Patiens Enrolled in the Collaborative Ocular Melanoma Study: COMS Report No 29. (2008) *Ophthalmology*; in press.
- 3 Collaborative Ocular Melanoma Study Group. Comparison of Clinical, Echographic, and Histopathological Measurements From Eyes With Medium-Sized Choroidal Melanoma in the Collaborative Ocular Melanoma Study: COMS Report No 21. (2003) *Arch Ophthalmol.* **121**: 1163–1171.
- 4 Virgili G. Gatta G. Cicollalo L (2007). Incidence of Uveal Melanoma in Europe. *Ophthalmology.* **114**: 2309–2315.
- 5 Isager P. Ehlers N. Overgaard J (2004). Prognostic factors for survival after enucleation for choroidal and ciliary body melanomas. *Acta Ophthalmol Scand.* **82**: 517–525.
- 6 Avery RB. Diener-West M. Reynolds SM (2008). Histopathologic Characteristics of Uveal Melanoma in Eyes Enucleated After Iodine 125 Brachytherapy in the Collaborative Ocular Melanoma Study. *Arch Ophthalmol.* **126**: 207–212.
- 7 Dibernardo C. Schachat A. Fekrat S (1998). *Intraocular Tumors. Ophthalmic Ultrasound A Diagnostic Atlas.* New York: Thiemes Medical Publisher. 87.
- 8 Nicholson DH. Byrne SF. Chiu MT. et all (1985). Echographic and histologic tumor measurements in uveal melanoma. *Am J Ophthalmol.* **100**: 454–457.
- 9 Folberg R. Gamel JW. Greenberg RA et all (1985) . Comparison of direct and microslide pathology measurements of uveal melanoma. *Incest Ophthalmol Vis Sci.* **26**: 1788–1791.
- 10 Collaborative Ocular Melanoma Study Group (1998). Histopathologic Characteristics of Uveal melanomas in Eyes Enucleated From the Collaborative Ocular Melanoma Study: COMS Report No 6. *Am J Ophthalmol.* **125**: 745–766.
- 11 Haritoglou C. Neubauer AS. Herzum H at all (2002). Interobserver and intraobserver variability of measurements of uveal melanomas using standardised echography. *Br J Ophthalmol.* **86**: 1390–1394.
- 12 Farah ME. Byrne SF, Huges JR (1984). Standardised echography in uveal melanomas with scleral or extraocular extension. *Arch Ophthalmol.* **102**: 1482–1485.
- 13 Coleman K. Baak JA. Van Diest P (1993). Prognostic factors following enucleation of 111 uveal melanomas. *Br J Ophthalmol.* **77**: 688–692.
- 14 Byrne SF. Green RL (1992). *Ultrasound of the Eye and Orbit.* Mosby Year Book, Inc. 505.
- 15 Baráková D (2002) . *Echografie v oftalmologii.* Praha: Professional Publishing.
- 16 Baráková D (2002). *Nitrooční tumory.* Grada Publishing, Praha.
- 17 Baráková D. Ředinová M (2001). Melanom cévnatky v echografickém obraze. *Čes. a slov. Oftal [Ultrasonography of Choroidal Melanoma (In Czech)].* **57**: 237–243.
- 18 Verbeek AM. Thijssen JM. Cuypers MHM (1994). Echographic classification of intraocular tumors. *Acta Ophthalmologica.* **72**: 416–422.
- 19 Rosa N. Cennamo G. Tranfa F (1992). Comparison between echographic and histological findings in choroidal malignant melanomas. *Acta Ophthalmologica. Supplement.* **204**: 99–101.
- 20 Scott IU. Murray TG. Huges JR (1998). Evaluation of Imaging Techniques for Detection of Extraocular Extension of Choroidal Melanoma. *Arch Ophthalmol.* **116**: 897–899.
- 21 Seddon JM. Albert DM. Lavin PT et all (1983). A prognostic factor study of disease-free interval and survival following enucleation for uveal melanoma. *Arch Ophthalmol.* **101**: 1894–1899.
- 22 Shamma HF. Blodi FC (1977). Orbita Extension of Choroidal and Ciliary Body Melanomas. *Arch Ophthalmol.* **95**: 2002–2005.
- 23 Byrne SR. Glaser JS (1983). Orbital tissue differentiation with standardised echography. *Ophthalmology.* **90**: 1071–90.
- 24 Marchini G. Tosi R. Ghimenton C (1997). Measurement of tumour height and base diameter in choroidal melanoma. Comparison between ultrasonography and histology. *Ultrasonography in Ophthalmology 15,* Kluwer Academic Publisher. Dodrecht. 93–100.